Defense Technical Information Center Compilation Part Notice

ADP011138

TITLE: Offset Piezoceramic Stack Actuators and Acceleration Feedback Control for Tail Buffet Alleviation of a High Performance Twin Tail Aircraft: Robustness Issues

DISTRIBUTION: Approved for public release, distribution unlimited

This paper is part of the following report:

TITLE: Active Control Technology for Enhanced Performance Operational Capabilities of Military Aircraft, Land Vehicles and Sea Vehicles [Technologies des systemes a commandes actives pour l'amelioration des performances operationnelles des aeronefs militaires, des vehicules terrestres et des vehicules maritimes]

To order the complete compilation report, use: ADA395700

The following component part numbers comprise the compilation report:
ADP011101 thru ADP011178

Offset Piezoceramic Stack Actuators and Acceleration Feedback Control for Tail Buffet Alleviation of a High Performance Twin Tail Aircraft: Robustness Issues

by

S. Hanagud, M. Bayon de Noyer,

Georgia Institute of Technology, School of Aerospace Engineering, Atlanta, Georgia 30332-0150

D. Henderson,

Air Force Research Laboratory

1950 Fifth Street

WPAFB, Ohio 45433 – 7251

Abstract

In high performance twin-tail aircraft, tail buffet occurs when unsteady pressures associated with separated flow excite the modes of the vertical fin structural assemblies. At high angles of attack, flow separates and is convected by the geometry of the wing-fuselage interface toward the vertical tails. This phenomenon, along with the aeroelastic coupling of the tail structural assembly, results in vibrations that can shorten the fatigue life of the empennage assembly and limit the flight envelope due to the large amplitude of the fin vibrations. The objective of this paper is to present a control system for buffet alleviation by the use of Offset Piezoceramic Stack Actuators (OPSA) in combination with acceleration feedback control. The emphasis of this paper is placed on the reliability and maintainability of the actuator and the robustness of the controller. The choice of actuator and controller is justified. Methods for the design and the placement of the OPSAs for tail buffet alleviation are elaborated. A method to design the acceleration feedback controller for tail buffet alleviation is presented. Finally, experimental validations of the effectiveness and the robustness of the controller are performed on a full-scale vertical tail sub-assembly and on a $1/16^{th}$-scale wind tunnel model.

Introduction

In a high performance twin-tail aircraft (HPTTA), buffet induced tail vibrations were first noticed through their destructive effects of induced fatigue cracks in the vertical tail structural assembly. In addition to the formation of fatigue cracks, buffet induced vibrations can restrict the flight maneuvering capability of the aircraft by restricting the angles of attack and speeds at which certain maneuvers can be executed. Because of these effects, a significant amount of maintenance efforts are spent on high performance twin-tail aircraft vertical tail assemblies in logistic centers. Buffet induced tail vibrations occur when unsteady pressures associated with separated flow, or when vortices, excite the vibration modes of the vertical fin structural assemblies. At high angles of attack, flow separates at the leading edge of the wings and vortices are generated at different locations such as the wing root or the leading edge extensions. These turbulent flows are convected by the geometry of the wing-fuselage interface toward the vertical tails. This phenomenon, along with the aeroelastic coupling of the tail structural assembly, results in vibrations that can shorten the fatigue life of the empennage assembly and limit the flight envelope due to large amplitudes of the fin vibrations.

Many different approaches to tail buffet alleviation have been investigated. These approaches can be divided into two sets, the aerodynamic methods[1-5] and structural dynamic methods. The structural dynamic approaches for buffet alleviation can also be divided into passive and active approaches. The passive structural method consists of reinforcing of the fin assembly with patches both to repair existing defects and to stiffen the assembly[6]. More recently, active structural dynamic approaches[7-18] have been developed. These methods use different types of actuators for buffet alleviation. The first type of actuator that was considered was an aerodynamic control surface[7,11,12], namely the rudder. Then, techniques based on smart structure concepts, which use active structural actuators, such as piezoceramic wafers[8-17] or stack assemblies[18] were investigated. Finally, a combination of the use of rudders for low frequencies and PZT wafers for higher frequencies has also been studied[16-17]. Simultaneously, controllers ranging from direct feedback[7] to neural predictive control have been studied[16].

The objective of this paper is to describe the results of our work in the area of buffet alleviation by the use of Offset Piezoceramic Stack Actuators (OPSA) in

Paper presented at the RTO AVT Symposium on "Active Control Technology for Enhanced Performance Operational Capabilities of Military Aircraft, Land Vehicles and Sea Vehicles", held in Braunschweig, Germany, 8-11 May 2000, and published in RTO MP-051.

combination with acceleration feedback control. The emphasis of this paper is placed on the reliability and maintainability of the actuator and the robustness of the controller. First, the choice of actuator and controller will be justified. Next, methods for the design and the placement of the OPSAs for tail buffet alleviation are elaborated. Third, methods to design the acceleration feedback controller for tail buffet alleviation are discussed. Finally, experimental validations of the effectiveness and the robustness of the controller are performed on a full-scale vertical tail sub-assembly and on a $1/16^{th}$-scale wind tunnel model.

Choice of Type of Actuator and Controller

Choice of Actuator

The selection criteria for the choice of vibration control actuator involve mechanical properties, electrical properties and cost. For tail buffet induced vibration suppression, the primary concern is the control authority that can be generated by the actuator. Comparisons between the use of the rudder or induced strain actuators for buffet alleviation by both Nitzsche et al.[11] and Moses[12] indicated that piezoceramic actuators are more efficient. Furthermore, as noted by Lazarus et al.[8], using induced strain actuators instead of the rudder enable the buffet alleviation system to run independently of the flight controls and hence does not restrict in any way the maneuverability of the aircraft.

For the purpose of buffet alleviation by induced strain actuation, every researcher[8-17], to date, has used Lead Zirconate Titanate (PZT) ceramic wafers as piezoelectric actuators. However, the control authority of PZT wafer actuators, unless used in large quantities, is usually not sufficient for this application. Stack actuators can increase the control authority through a more efficient use of the piezoceramic material properties. This increase is obtained by the use of the longitudinal d_{33} coefficient instead of the transverse d_{31} or d_{32} coefficient generally used with wafers. Furthermore, the increased stack strain results from the addition of the effective piezoelectric elongation of each PZT layer in series.

Piezoceramic stack actuators have been successfully used for vibration control. This type of actuator has been used, as active elements for vibration suppression, in truss structures[19]. These actuators have also been used to generate point loads to control vibrations in plates by placing them between the plate and a stiffener[20]. Furthermore, piezoceramic stack actuators have been implemented as moment inducing actuators by placing the stack within cutouts in stiff beams and plates[21] or mounting the stack in an external assembly for vibrations suppression in rapid fire guns[22].

These concepts have been the motivation for the choice of an actuator in this research program. Piezoceramic stack actuators can be used as "induced bending moment actuators", which can generate much larger moments than PZT wafers. For this research program, an externally mounted actuator sub-assembly was designed, this actuator was called the "Offset Piezoceramic Stack Actuator" (OPSA). This OPSA was designed to have enhanced reliability and maintainability properties compared to previously designed piezoceramic stack based actuators. For active buffet alleviation, this piezoceramic stack actuator structural assembly would be bonded to the vertical tail skin and covered by aerodynamic shielding if necessary.

Choice of Controller

Previous investigations, in the field of buffet alleviation, have used different types of controllers ranging from direct feedback[7] to neural predictive control have been studied[16]. These different methods have some advantages and some drawbacks. For example, one of the problems associated with the use of an LQG controller is that it requires an accurate model for both the structure and the loads because the design of its observer depends on the external load influence matrix. Further, LQG controllers do not provide guaranteed robustness properties.

For the problem of buffet alleviation, the loads have not, to date, been accurately modeled. As a result, some of the control designs have used methods of identifying the load profile by using wind tunnel data[7], while others have used a "linearized" concept which models the aeroelastic buffeting behavior of the tail as a superposition of two independent mechanisms (unsteady airloads induced by structural oscillations and the driving airloads due to buffeting)[11].

Another significant problem associated with most controllers is their spillover effect. Spillover effects are the result of both sensing and actuating the unmodeled or uncontrolled modes or states of the controlled structure. These spillover effects will introduce changes between the modeled closed loop result and the actual behavior of the closed loop system. These changes may even result in instabilities. To decrease the spillover effects, it is important that the magnitude of the controller transfer function decrease rapidly as frequency increases which means that the controller has a fast roll-off at high frequencies that include unmodeled modes. Furthermore, for non-collocated accelerometers and actuators, the phase of the controller signal should be either 0 or 180 degrees, with respect to the sensor signal, at high frequencies such that the control forces do not drive the structure unstable by decreasing the closed loop damping.

Another problem is the order of the controller, which is significant for its implementation. The order of the controller, when implemented digitally, is directly related to the rate at which the controller can be implemented and the size of the code which must be stored in the memory on the controller system. This means that for large order controllers, their implementation cannot be executed rapidly and will require a large amount of memory.

In classical approaches to the control of flexible structures, system equations are usually rewritten in a state space domain. But these transformations to state space domain often lose insight into the physics of the problem from the point of view of a structural dynamicist. Since the work of Goh and Caughey[23] with the introduction of the Positive Position Feedback (PPF) controller, second order compensators enable designers to keep the system of equations of motion in their second order form. However, control schemes such as PPF and Strain Rate Feedback (SRF) are not unconditionally stable. Juang and Phan[24] proposed a second order compensator using acceleration feedback, that was unconditionally stable. The unconditional stability of the scheme, applied to flexible structure, was later proved for multiple pairs of collocated sensors and actuators with their actuator dynamics[25]. In 1996, Goh and Yan[26] developed a method of assigning the damping ratio and scalar gain to these pairs of collocated sensors and actuators which was based on the use of critically damped compensators. Then, Bayon de Noyer and Hanagud[27] have shown that the acceleration feedback control can also be applied to non-collocated actuators and sensors with stability restrictions. They further developed two methods[28] to obtain the parameters of the compensators for both single mode and multi-mode control using a single actuator or a single actuator array, one based on crossover point design and one based on the H_2 optimization of the closed loop transfer function.

As illustrated in the different designs[26-28] for Acceleration Feedback Control (AFC), the computation of the controller parameters does not require the external load influence matrix. As a result, the controller design does not require an accurate model of the loads. Further, AFC has a relative degree of two between the denominator and numerator of each of the controller transfer functions of two so that its roll-off at high frequencies is 40dB per decade and its phase at those frequencies is either 0 or 180 degrees, which is beneficial for non-collocated actuators and sensors. Furthermore, AFC enables the designer to control the vibration amplitude at selected frequencies within a given bandwidth without increasing the order of the controller for uncontrolled states. Finally, the equations of motion of the closed loop system and of the controller can be written in a similar second order equation form.

Offset Piezoceramic Stack Actuator

Actuator Design

The main challenge, associated with the use of stacked piezoceramic actuators in tail buffet alleviation, is that a piezoceramic stack produces only longitudinal motion or forces. Hence, an assembly was designed to transform the longitudinal motion of the stack into moments that will produce the control actuation. Such a transformation was achieved by placing the piezoceramic stack parallel to the controlled structure at a distance from its neutral axis and at a selected orientation. This distance creates a lever arm so that the longitudinal forces results in local moments on the structure.

This new high authority actuator assembly is made of two blocks bonded to the structure to provide an offset distance from the surface of the system to be controlled. A piezoceramic stack is placed between these two blocks and pre-compressed using a bolt. This pre-compression is necessary because the actuator can only provide control moments while extending from its rest position. By pre-compressing the active element, an offset stress is created that will enable the piezoceramic stack to provide control moments over almost the full control cycle. Furthermore, before any control signal is applied, the active element is also electrically pre-compressed by applying a DC bias. This design is illustrated in Figure 1.

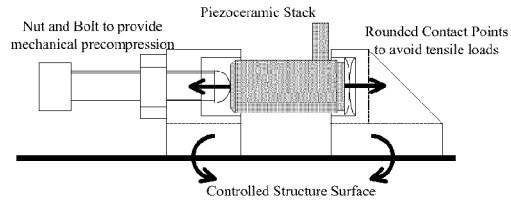

Figure 1. Offset Piezoceramic Stack Actuator

Reliability benefits associated with the offset piezoceramic stack actuator are as follows. Since the piezoceramic stack is only compressed between the two blocks of the assembly, tensile loads are not transmitted to the active element. This fact reduces the possibility of actuator failure. Furthermore, in this design, the rounded point contacts between the piezoceramic stack and the mounts insure that bending loads are not transmitted to the active element as well, which reduces even further the possibility of stack failure in local tension. It is to be noted that, for maintainability, the bolt is used to permit an easy removal of the piezoceramic stack while the actuator assembly is bonded to the system to be controlled. Hence, if failure were to occur, the active element could be replaced easily during regularly scheduled maintenance.

For large amplitude vibration suppression, the primary concern is the control authority that can be generated by the actuator. To obtain a maximum control authority, the resultant forces that the actuator develops should be as large as possible. However, the power requirement of the actuator increases with the maximum authority that the active element can deliver. To produce the needed control moments, the active element of the Offset Piezoceramic Stack Actuator can be chosen from different types of piezoceramic stacks. Low-voltage (100V) piezotranslators can generate blocked force in the range of 180N to 3kN while high-voltage (1000V) piezotranslators can generate blocked force in the range of 1.5kN to 30kN. Once the type of the piezoceramic

stack has been selected, the dimensions of the offset piezoceramic stack actuator assembly should be computed such that the chosen active element fits within the mount and optimal actuation energy transfer is obtained.

Actuator Offset and Placement Optimization

For controller design purposes, the modal influence matrix of the actuators is required to model the plant in the modal space. To obtain such a matrix for a complicated structure, a FEM model of the system should be developed. However, during this research work, to test the reliability of the finite element model of the OPSA and to gain insight into the physics of the actuator, an analytical solution for a simple structure was developed. The simple system studied was a steel cantilever beam, which was 24-in long, 0.5-in thick and 2-in wide. An offset piezoceramic stack actuator (OPSA) was bonded on the upper surface of the beam close to its clamped end. The OPSA was made of two steel blocks bonded to the cantilever beam with a piezoceramic low-voltage translator, Physik Instrumente PI-830.10, clamped between the blocks.

A modal expansion based model was developed to model the actuation of the OPSA on an Euler-Bernoulli beam with a torsional spring support on one end and free at the other end. Then, an optimization of the actuator placement and of the vertical offset distance was derived based on this model. Given the active element of the OPSA, namely the piezoceramic stack, the objective of this optimization was to maximize the control authority of the offset piezoceramic stack actuator for the control of vibrations of the cantilever beam. For acceleration feedback control, the control sensor optimal location on a cantilever beam is the free tip. In such a case all of the modal influence coefficients of the accelerometer are maximum. In order to maximize the control authority of the control system, we need to optimize the actuator authority of the OPSA. This means that we should maximize the modal influence coefficients of the OPSA for the modes that have been selected for control.

If the length of the actuator is small compared to the beam length, we can make the following two approximations. First, the natural frequencies of the actuated beam are independent of the vertical offset distance and actuator position. Second, the mode shapes of the actuated beam are also independent of the vertical offset distance and actuator position. These two approximations combined insure that an approximation of the optimal vertical offset distance would be the same for every mode and that the placement analysis can be performed on the structure without any actuator mounted. In this case, we take the derivative of any modal influence coefficient of the OPSA with respect to the vertical offset distance and set this derivative to zero. We obtain that the offset distance is optimal when the added bending stiffness due to the piezoceramic stack matches the bending stiffness of the beam alone. So that:

$$\delta_{opt} = \sqrt{\frac{E_b I_b}{A_s Y^E_s}} \qquad (1)$$

Where δ_{opt} is the optimal vertical offset, E_b and I_b are the Young's modulus and Moment of Inertia of the beam, and A_s and Y^E_s the cross sectional area and Young's modulus of the piezoceramic stack.

The placement of the actuator is based on reciprocity theory. The principal mode of actuation, which is induced by the offset piezoceramic stack actuator, is the input of a pair of bending moments in opposite directions located at the end mounts locations on the beam. The objective of the placement optimization is to obtain maximum transverse acceleration at the sensor location, the free tip of the cantilever beam, due to the pair of moments. By reciprocity theory, this optimization is equivalent to finding the locations with maximum curvature due to an input of transverse disturbance force located at the sensor position. As discussed before, if the length of the actuator is small compared to the beam length, the placement analysis can be performed on the structure without any actuator mount.

For a more complex structure, such as a vertical tail, the optimal offset distance can be obtained by matching the bending stiffness due to the piezoceramic stack with the local bending stiffness of the structure. Further, in order to obtain optimal placement of the actuator, an experimental method is developed. The optimization is performed such that local moments, which are induced by the offset piezoceramic stack actuators, produce maximum response from the control sensor. As discussed above and as illustrated in Figure 2, using reciprocity theory, the actuators are placed at the locations and in directions where the curvature responses due to a disturbance force at the sensor location, in the measured direction, are maximum.

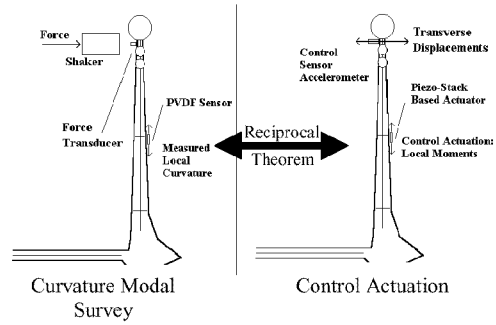

Figure 2. Principles of Actuator Placement

Since the actuators are bonded on the surface of the controlled structure, a local two-dimensional approximation of the system is assumed. This approximation means that, at each actuator location, the structure is supposed to behave like a two-dimensional

system. As a result, a curvature modal survey is performed in the neighborhood of candidate locations to obtain optimal placements of the actuators. The curvature modal survey is an experimental modal analysis, in which, instead of measuring acceleration, curvature is measured in three directions, due to the local two-dimensional approximation of the structure, at each point. This analysis is performed by disturbing the structure at the control sensor location and in the measurement direction. Then, the response from a curvature sensor, such as a PVDF film, is measured in the immediate area of each candidate actuator location in three different directions. From the three measured curvatures at a set of locations, the optimal location and optimal orientation of the actuator is obtained.

Acceleration Feedback Control

Acceleration feedback control (AFC) is based on measuring acceleration and applying a second order compensator to the sensor signal to obtain control forces. The equations of motion of the closed loop system and of the controller are in a second order equation form, as is illustrated in the following equation.

$$\begin{aligned} &[M]\{\ddot{x}\}+[C]\{\dot{x}\}+[K]\{x\}=-[\Gamma_{act}][G][\Omega_c]\{\eta\}+\{f\} \\ &\{\ddot{\eta}\}+[\Lambda_c]\{\dot{\eta}\}+[\Omega_c]\{\eta\}=\{1_p\}[\Gamma_{acc}]\{\ddot{x}\} \end{aligned} \quad (2)$$

In the above equations, $\{x\}$ is the vector of degrees of freedom of the system, $\{\eta\}$ is the vector of the p compensator coordinate, $[\Gamma_{act}]$ is influence matrix of the actuators, $[\Gamma_{acc}]$ is influence row vector of the accelerometer, $[\Lambda_c]$ is the compensator damping matrix and $[\Omega_c]$ is the compensator frequency matrix, [G] is the feedback gain matrix and $\{1_p\}$ is a vector of length p, with one for each entry, to account for the fact that all compensators are placed in parallel.

Single Degree of Freedom AFC

The generalized equations describing the closed loop behavior of a single degree of freedom system under Acceleration Feedback Control (AFC) consist of a structural equation with a feedback force due to the actuator and a disturbance force, and a compensator equation with acceleration sensing. These equations are generalized by introducing influence parameters for the actuator and for the sensor. These equations, in the modal space, are:

$$\begin{cases} \ddot{\xi}+2\zeta_s\omega_s\dot{\xi}+\omega_s^2\xi=-a_1\gamma\omega_c^2\eta+f \\ \ddot{\eta}+2\zeta_c\omega_c\dot{\eta}+\omega_c^2\eta=a_2\ddot{\xi} \end{cases} \quad (3)$$

In these equations, ξ and η are the modal coordinates of the structure and of the compensator; respectively. Then, ω_s, ω_c, ζ_s and ζ_c are the natural frequencies and the damping ratios of the structure and the compensator, respectively. Further, γ is the controller gain applied to the feedback signal; and a_1 and a_2 are the influence parameters of the actuator and sensor, respectively. Finally, f is the external disturbance that drives the system.

Without loss of generality, by taking the Laplace Transforms of Equation (3), assuming zero initial conditions, and solving for η, the transfer functions of the closed loop system and of the controller, are obtained:

$$\begin{cases} G_s(s)=\dfrac{\overline{\xi}}{\overline{f}}=\dfrac{\left(s^2+2\zeta_c\omega_c s+\omega_c^2\right)}{\left(s^2+2\zeta_s\omega_s s+\omega_s^2\right)\left(s^2+2\zeta_c\omega_c s+\omega_c^2\right)+a_1a_2\gamma\omega_c^2s^2} \\ G_c(s)=\dfrac{\omega_c^2\gamma\overline{\eta}}{a_2s^2\overline{\xi}}=\dfrac{\omega_c^2\gamma}{\left(s^2+2\zeta_c\omega_c s+\omega_c^2\right)} \end{cases} \quad (4.a\text{-}b)$$

Equation (4.b) shows that the controller has a relative degree of two between its denominator and numerator. This results in a controller with 40 dB per decade roll-off and a phase of 0 or 180 degrees at high frequencies.

The stability of such a system can be studied by applying the Routh-Hurwitz criterion[48] to the closed loop characteristic equation:

$$\left(s^2+2\zeta_s\omega_s s+\omega_s^2\right)\left(s^2+2\zeta_c\omega_c s+\omega_c^2\right)+a_1a_2\gamma\omega_c^2s^2=0 \quad (5)$$

For the purpose of this analysis, the open loop system and the controller are assumed to be asymptotically stable. Then, if a_1 and a_2 have the same sign, meaning that the mode is observed in phase by the sensor with respect to the actuator input, a sufficient condition for stability is that γ is positive. On the other hand, if a_1 and a_2 have opposite signs, meaning that the mode is observed out of phase by the sensor with respect to the actuator input, a sufficient condition for stability is that γ is negative. Since the only term depending on γ always appears in the form $a_1a_2\gamma$ in Equations (5), a sufficient condition for stability is that $a_1a_2\gamma$ be positive.

Design of the AFC Parameters for a SDOF System based on the Optimization of the H_2 Norm of the Closed Loop Modal Receptance

In the case of vibration suppression in a given structure, an optimization of the controller design parameters can be performed to meet a selected objective or a performance criterion. One way to design the single degree of freedom AFC compensator for vibration suppression is to minimize the H_2 norm of the closed-loop receptance which is the system transfer function, $G(j\omega)$, between the modal displacement and the external disturbance force. The performance criterion is defined to be:

$$\begin{aligned} \|G\|_2 &= \left(\frac{1}{2\pi}\int_{-\infty}^{+\infty} \|G(j\omega)\|_F^{\,2}\, d\omega \right)^{1/2} \\ &= \left(\int_0^{+\infty} \|H(t)\|_F^{\,2}\, dt \right)^{1/2} = \|H\|_2 \end{aligned} \quad (6)$$

In this Equation, H is the impulse-response matrix of the system, which is the inverse Laplace transform of the transfer function matrix.

This design is equivalent to minimizing the L_2 norm of the impulse modal response of the closed loop system due to a unit impulse load. Or for a stochastic process, this design is equivalent to minimizing the covariance of the closed loop modal response due to a unit white noise disturbance. It is to be noted that none of the definitions depends on the control signal directly. Hence, on the basis of this criterion, the controller will be a high authority controller. For this design, it will be proved that there does not exist an optimal controller gain. Therefore, instead of defining the controller gain by weighting the control signal, it can be defined by iterations in such a way that the control signal is not saturated.

To optimize the acceleration feedback control compensator for the norms defined in Equation (6), we define a functional J, which depends on the controller parameters:

$$J(\omega_c,\zeta_c,\gamma)=\|G\|_2^{\,2} \tag{7}$$

The closed loop system can be rewritten in a state space based on the modal states of the controlled system and the controller states:

$$\begin{cases}\dot{x}(t)=\tilde{A}x(t)+\tilde{B}w(t)\\ y(t)=\tilde{C}x(t)\end{cases} \tag{8}$$

where:

$$x=\left[\xi \quad \dot{\xi} \quad \eta \quad \dot{\eta}\right]^T$$

$$\tilde{A}=\begin{bmatrix}0 & 1 & 0 & 0\\ -\omega_s^{\,2} & -2\zeta_s\omega_s & -a_1\gamma\omega_c^{\,2} & 0\\ 0 & 0 & 0 & 1\\ -a_2\omega_s^{\,2} & -2a_2\zeta_s\omega_s & -(1+a_1a_2\gamma)\omega_c^{\,2} & -2\zeta_c\omega_c\end{bmatrix}$$

$$\tilde{B}=\left[0 \;\; 1 \;\; 0 \;\; a_2\right]^T \text{ and } \tilde{C}=\left[1 \;\; 0 \;\; 0 \;\; 0\right] \tag{9}$$

The functional defined in Equation (8) is then given by:

$$J(\omega_c,\zeta_c,\gamma)=\mathrm{tr}\left(\tilde{B}^T P\tilde{B}\right)=\mathrm{tr}\left(P\tilde{B}\tilde{B}^T\right) \tag{10}$$

Where, since the closed loop system is assumed to be stable, P is the observability Gramian of the closed loop system, which is the positive definite solution of the Lyapunov equation:

$$P\tilde{A}+\tilde{A}^TP+\tilde{C}^T\tilde{C}=0 \tag{11}$$

Since P is symmetric, its 10 independent elements are obtained by solving the linear system of equations given by Equation (11). Then by computing the trace of the product of matrices defined by Equation (10), the H_2 norm of the transfer function between the modal response and the external disturbance is obtained. Then, the derivative of the norm with respect to ω_c, ζ_c and γ are set to zero. First, we obtain that the derivative with respect to γ that is strictly negative and increases uniformly toward zero as γ tends to infinity. Hence, there is no optimal solution for the controller gain as a design parameter.

However, for a particular controller gain, the following condition, to minimize the H_2 norm, is obtained:

$$\zeta_c\left(\frac{\omega_c^{\,2}}{\omega_s^{\,2}}-1\right)\left(\frac{\omega_c^{\,2}}{\omega_s^{\,2}}+2\frac{\zeta_c}{\zeta_s}\frac{\omega_c}{\omega_s}+1\right)=0 \tag{12}$$

In order to obtain a ratio between the natural frequency of the controller and the natural frequency of the open loop system that is real and positive, the only possible condition is:

$$\omega_c=\omega_s \tag{13}$$

With this condition, the second equation that should be satisfied to minimize the H_2 norm of the closed loop transfer function is as follows:

$$(\zeta_c+\zeta_s)^2\left(a_1a_2\gamma-4\zeta_c^{\,2}\right)=0 \tag{14}$$

For a stable controller, the compensator damping ratio should be positive. Hence, the only possible solution of Equation (14) is:

$$\zeta_c=\frac{1}{2}\sqrt{a_1a_2\gamma} \tag{15}$$

It is to be noted that for this design to meaningful, the controller damping ratio should be real. Hence, the product $a_1a_2\gamma$ must be positive and the closed loop system will be stable.

As a result, the design of an AFC controller that minimizes the H_2 norm of the closed loop transfer function between modal displacement and external load of an SDOF system begins with the choice of a controller gain such that the product $a_1a_2\gamma$ is positive. Then, Equation (15) is used to compute the optimal damping ratio for the controller. Finally, the natural frequency of the controller is set to be equal to the natural frequency of the open loop system. In order to insure that the control signal will not be saturated, closed loop simulations can be investigated and an iteration process on the controller gain can be performed.

Uncertainties and Robustness

The principal drawback associated with the use of optimal controllers arises from uncertainties in the model of the open loop system, which will create departure from optimality and may even lead to instabilities. As discussed previously, a sufficient condition for stability is that the product $a_1a_2\gamma$ is positive. Hence, the only uncertainties that may lead to instability are uncertainties in the sign of the product of the actuator and sensor influence coefficients, a_1a_2. However, such type of uncertainty are extremely unlikely since the phase of the modeled transfer function

is defined by this product and can be easily compared to the phase of the actual transfer function between the control sensor and the actuator input voltage. Hence, robust stability of the H_2 optimal design for a single degree of freedom system is insured.

To study the effect of uncertainty on the performance of the H_2 optimal design, the departure from optimality due to uncertainties in the open loop system parameters is studied. Since the open loop parameters are scalars, any type of linear uncertainty can be modeled as:

$$q_{s,true} = q_{s,identified}\left(1+\varepsilon_q\right) \tag{16}$$

The uncertainties are defined to be present in the natural frequency, ε_ω, the damping ratio, ε_ζ, and the product of the sensor and actuator influence coefficients, ε_a.

The departure from optimality due to uncertainties, D_{opt}, is defined as the difference between the H_2 norms of the closed loop system using controller parameters computed with the identified uncertain modal parameters and the H_2 norms of the closed loop system using controller parameters computed with the actual parameters normalized by the latest. Hence, the departure from optimality due to uncertainties is defined to be:

$$D_{opt} = \frac{\left\| G_{cl,\text{controller based on identified parameters}} \right\|_2 - \left\| G_{cl,\text{controller based on true parameters}} \right\|_2}{\left\| G_{cl,\text{controller based on true parameters}} \right\|_2} \tag{17}$$

By assuming small uncertainties, meaning all ε's small with respect to one ($\varepsilon \ll 1$), and then a small open loop damping ratio, since typical damping ratios are less than 0.05, a Taylor series approximation, of order two, of the departure from optimality is given by:

$$D_{opt} \approx \frac{1}{4}\left[\left(1-\frac{3}{2}\alpha\left(1+\varepsilon_\zeta\right)\right)\varepsilon_a + \left(1-\frac{5}{2}\alpha+\frac{\alpha^2}{\zeta_s{}^2}\left(1-\frac{7}{2}\alpha\right)\right)\varepsilon_\omega{}^2 + \frac{1}{4}\left(\frac{3}{2}\alpha-1\right)^2\varepsilon_a{}^2\right] + O\left(\varepsilon^3\right) \tag{18}$$

In this equation, the non-dimensional parameter α is the ratio between the open loop damping ratio and the controller damping ratio computed for the model. It is given by $\alpha = 2\zeta_s \Big/ \sqrt{a_1 a_2 \gamma}$. For most applications, the parameter α is chosen to be larger than the open loop damping ratio, ζ_s, to obtain a less than critically damped compensator.

We can assess from Equation (18) that, for a large compensator gain ($\alpha \ll 1$), the departure from optimality due to uncertainties in the model of the sensor and actuator influence parameters behaves like ε_a. This means that a controller with actual influence parameters larger than the one modeled will likely perform better than expected. Simultaneously, the departure from optimality associated with uncertainties in the damping ratio of the open loop system decreases when the value of the controller gain is large. This also applies to the case of the uncertainties in natural frequency. Furthermore, to keep the departure from optimality due to uncertainties in the natural frequency small, the coefficient multiplying $(\alpha/\zeta_s)^2$ in Equation (18) should be positive. Hence α should be kept below 2/7. This means that the minimum value of the gain that should be chosen for the controller is $\gamma_{min} = 49\zeta_s{}^2 / a_1 a_2$.

AFC H_2 Norm Optimization of the Closed Loop Modal Response Design for Multi-Input, Single-Output Systems

The optimal controller design for multi-input, single-output systems is divided into three steps. The first step consists of choosing the output measurement vector and the controller gain matrix. The choice of the output measurement vector means the choice of modal weighting. When the output measurement vector is defined, a controller gain matrix should be defined in such a way that each entry of the 1 x n_c vector given by the product $\left[\tilde{\Gamma}_{acc}\right]\left[\tilde{\Gamma}_{act}\right][G]$ is positive. In the particular case where no mode is controlled by more than one actuator array, this condition is equivalent to insuring that the product $a_1 a_2 \gamma$ is positive for every controlled mode. Hence, as discussed previously, this restriction on the gain matrix is given to insure that under the assumption that the structural closed loop system is uncoupled, the system is stable.

The second step of the numerical optimization consists in the definition of some initial guess for the optimal controller natural frequencies and damping ratios. This definition is performed under the assumption that the closed loop system can be uncoupled in a set of uncoupled structural modes under acceleration feedback control and a set of uncoupled and uncontrolled structural modes. Under this assumption, the parameters of each of the controller second order compensator can be computed independently based on the formulas given in the single degree of freedom design section depending on the choice of weight matrices.

The final step of the optimization procedure computes the optimal natural frequencies and damping ratios for the controller. In this research work, the numerical minimization is performed using the fmins function of the Matlab software in which the minimization is performed using the Nelder-Mead simplex search which is a direct search method that does not require gradients or other derivative information. In order to complete the step, the H_2 norm criterion should be computed. This computation is completed in three steps. First, at each iteration of the optimization, the closed loop system state matrix, A_{cl}, and the closed loop input disturbance matrix, B_{cl}, are computed. The choice of the output measurement vector defines the output performance measurement matrix, C_{cl}. Then, the optimization criterion, J, given by the H_2 norm of the performance measurement for a unit white noise

disturbance, is defined to be, as a function of the observability Gramian, P, as follows:

$$\|z\|_2 = J(\{\omega_c\},\{\zeta_c\}) = \left[tr\left(B_{cl}{}^T P B_{cl}\right)\right]^{1/2} \quad (19)$$

Since, the closed loop system is assumed to be stable, the observability Gramian of the closed loop system, P, is positive definite and is the solution of the Lyapunov equation:

$$PA_{cl} + A_{cl}{}^T P + C_{cl}{}^T C_{cl} = 0 \quad (20)$$

Hence, the second step of the computation of the optimization criterion consists in solving Equation (20) for the observability Gramian, P. Then, the last step of the computation consists of evaluating Equation (19) for the optimization criterion.

Wind Tunnel Tests

To validate the use of AFC in reducing the buffet-induced vibrations of the vertical tails of an HPTTA and the associated robustness, a 1/16th-scale wind tunnel model, shown on Figure 3, was designed and built. This model consisted of a rigid fuselage and wings with an aeroelastically scaled empennage.

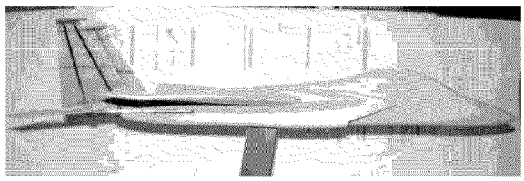

Figure 3. Scaled model of the HPTTA

The wind tunnel tests were performed at the Georgia Tech Research Institute Model Test Facility (GTRI-MTF). The GTRI-MTF wind tunnel is a closed-return, atmospheric, low-speed wind tunnel that has a rectangular test section 30 inches high and 43 inches wide with a usable length of 90 inches. This facility is capable of empty tunnel speeds of up to 200 ft/sec and corrected maximum dynamic pressures of 50 psf. During the tests wall corrections were not considered for the following reasons. The vortices, which are responsible for the buffet, are formed near the junction of the fuselage, the engine inlets and wing leading edges. Furthermore, the tail sub-assembly, where the measurement of buffet loads are obtained, are near the center of the tunnel cross section. Because blockage correction factors for separated flow were not available, the free stream dynamic pressure was corrected by using approximate correction factors that were obtained from flows at low angles of attack.

Results from preliminary wind tunnel tests, MacAir experiments reported by Triplett[29] and earlier Georgia Institute of Technology tests reported by Komerath et al.[30] showed that there exists a characteristic frequency associated with the maximum buffet load and that its associated reduced frequency is almost the same for all experiments. Hence, we determined that it was very important for the active tail buffet alleviation tests to scale the model such that the reduced frequencies are conserved. To operate in the middle of the optimal range for the Georgia Tech Research Institute Model Test Facility (GTRI-MTF) wind tunnel, the scale model of the empennage was designed to have natural frequencies 2.25 time larger than the full-scale tail sub-assembly. This model would then operate at a free stream dynamic pressure of 9 psf to conserve the reduced frequencies of the flow and structure. This dynamic pressure was equivalent to a free stream velocity of 26.9 m/s that translates approximately (because of compressibility effects) to a free stream velocity of 191.5 m/s for the full-scale aircraft or about Mach 0.6 at 20,000 ft.

The main objective of the wind tunnel tests was to demonstrate our ability to suppress all the principal modes of the HPTTA vertical tails that participate in the buffet response at high angles of attack. In addition, to demonstrate the robustness of the control system, it should not only perform well at the angle of attack corresponding to the worst buffet conditions but also over a wide range of angles of attack and free stream dynamic pressure. Hence, to validate the controller, different experiments were conducted. First, a control experiment is run at the predetermined worse buffet condition of 20 degrees angle of attack and 9 psf of free stream dynamic pressure. Then four different angles of attack were selected and the free stream dynamic pressure was varied from 5 to 13 psf.

To locate the sensor for the control experiments, three conditions dictated the placement. First, the vertical tails of our model behaves like a cantilever tapered plate. Second, the sensor, which is generally used for acceleration feedback control, is an accelerometer. Third, to maintain the vortex cohesion, minimum flow disturbance due to the sensor should be obtained. As a result, the optimum location for the sensor was on the trailing edge tip of the vertical tail. The placement was validated experimentally to check that all modes in the control range were observable.

The next phase was to determine at which attitude the worse disturbances are encountered. Since we assume linearity of the structure, the dynamic response of the vertical tail was measured instead of the pressure. First, a fine survey was conducted for angles of attack ranging from 0 to 23 degrees, which showed that the angle of attack that displays the maximum tip response was approximately 20 degrees. This agrees with the results reported by Komerath et al.[30] during their tests. However, it does not agree exactly with the results of Triplett[29]. He reported a worse case at an angle of attack of 22 degrees.

At this point, the left vertical tail was instrumented with two pairs of offset piezoceramic stack actuators. The first pair of actuators was located to obtain large bending actuation authority and was bonded at the root

of the vertical tail along its mid-chord line. The second pair of OPSA actuators was placed for torsion control and was bonded at 35 degrees with respect to the mid-chord line above the first pair. This configuration is illustrated by Figure 4.

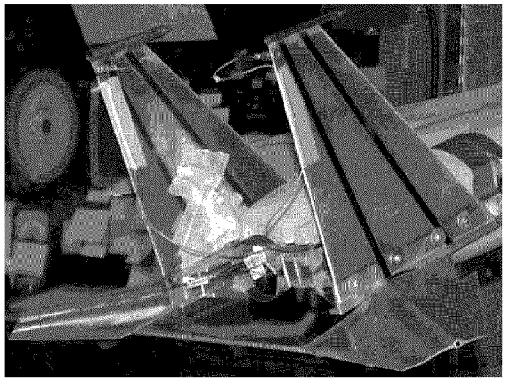

Figure 4. Active Buffet Alleviation Experiment Vertical Tails with OPSA Actuators.

Then, to assess the authority of the actuator arrays, the auto-power spectrum of the dynamic response of the control sensor excited by the buffet vortices was compared with the auto-power spectrums of the actuator arrays converted from the experimental transfer functions of the plant for a flat maximum input voltage. This operation showed that enough actuator authority was attained.

The next task associated with designing a controller was to obtain a mathematical representation of the system to be controlled. This representation is usually referred to as a "plant". To obtain the plant model, experimental transfer functions were obtained between the input voltage to each actuator array and the control sensor response voltage. Then, using a combination of system identification techniques such as single pole fitting and complex circle fitting around the poles, the parameters of each of the transfer functions were extracted.

Once the plant model had been developed and the actuator authority checked, the controllers were designed. For this experiment, the type of controller that was selected was acceleration feedback control (AFC). And the type of design for AFC that was used was the H_2 optimization of the closed loop transfer function design. Two different controllers were designed, one for the bending array and one for the torsion array. A single degree of freedom compensator was designed for each mode using the parameters extracted earlier. In order to avoid clipping of the control signal, the damping of each compensator was chosen to be seven times larger than the damping of the associated mode. Once the controllers were designed, their stability and effects on other modes were checked using root locus plots. Since root locus plots did not show any instability and each controller did not affect the parameters of the other controller, the controllers could be implemented simultaneously.

The controllers were implemented on a dSPACE system based on a digital signal processor (DSP). The coding of the overall control experiment was done using block programming with the Matlab extension called Simulink. The file was then converted to the DSP machine language and downloaded to the dSPACE system. Once the system started, the controllers were active.

To validate the controllers, three different experiments were carried out. First, a control experiment was run at the predetermined operating condition of 20 degrees angle of attack and 9 psf of free stream dynamic pressure. The auto-power spectrums of the uncontrolled and controlled trailing edge tip acceleration are illustrated in Figure 5. This figure shows that each of the controlled frequency has its auto-power spectrum reduced by a factor of at least 5. Furthermore, in the case of the first bending mode and second torsion mode, the responses are suppressed to a level equivalent to the one that would be obtained in the absence of these modes.

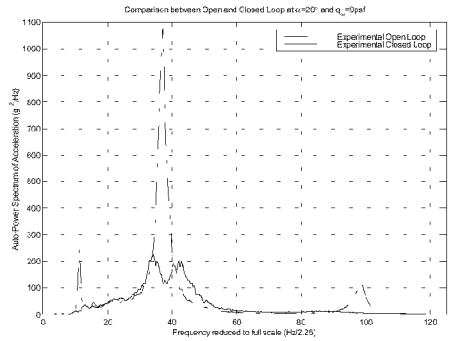

Figure 5. Comparison Between Open and Closed Loop Auto-Power Spectrum of Trailing Edge Tip Acceleration at θ=20° and q_∞=9psf.

Once the controller had been validated at its operating point, its effectiveness and robustness had to be checked at different conditions. For the second experiment, the operating free stream dynamic pressure of 9 psf was kept. However, the angle of attack was varied from 0 to 23 degrees. This control experiment showed that the root mean square of the trailing edge tip acceleration was reduced by up to 30% below 15 degrees and by about 20% at 20 degrees. This experiment also showed that the controllers were effective on the whole range of angles of attack.

Finally, four different angles of attack were selected. 14, 17, 20 and 23 degrees angles of attack cover the different regimes of buffet that the scaled model was encountering. For each angle of attack, the

free stream dynamic pressure was varied from 5 to 13 psf. As before, the results showed that as the disturbance increases the effectiveness of the controllers decreases. However, even at a free stream velocity 25% higher than the operating free stream velocity, the minimum RMS reduction was still 17%. These results, illustrated in Figure 6, prove that the controllers were stable and effective over the full buffet domain which means angles of attack ranging from 14 to 23 degrees and free stream velocity ranging from –25% to +25% of the full-scale equivalent of Mach 0.6 at 20,000 ft.

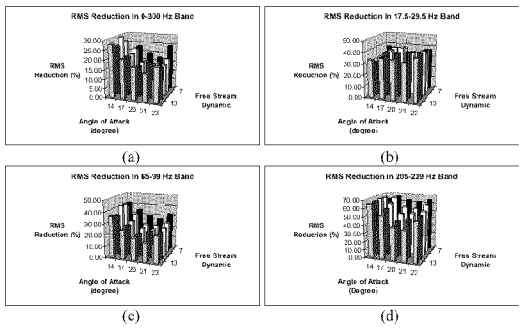

Figure 6. Percent RMS reduction in (a) the control bandwidth, (b) about the first bending mode, (c) about the first torsion mode, (d) about the second bending mode.

Conclusion

The objective of this paper was to present a robust control system for buffet alleviation by the use of Offset Piezoceramic Stack Actuators (OPSA) in combination with acceleration feedback control. The choice of actuator and controller was justified. Methods for the design and the placement of the OPSAs for tail buffet alleviation were elaborated. A method to design and study the robustness of the acceleration feedback controller for tail buffet alleviation was presented. Finally, experimental validations of the effectiveness and the robustness of the controller were presented on a full-scale vertical tail sub-assembly and on a 1/16th-scale wind tunnel model.

References

[1] Hebbar, S.K., Platzer, M.F., and Frink, W.D., "*Effect of Leading-Edge Extension Fences on the Vortex Wake of an F/A-18 Model*", J. of Aircraft, v. 32, n. 3, 1995, pp 680-682.

[2] Klein, M.A., and Komerath, N.M., "*Reduction of Narrow-Band Velocity Fluctuation Over an Aircraft Model*", 15th Applied Aerodynamic Conf., 1997, AIAA 97-2266.

[3] Bean, D.E., and Wood, N.J., "*Experimental investigation of twin-fin buffeting and suppression*", J. of Aircraft, v. 33, n. 4, 1996, pp. 761-767.

[4] Gee, K., Rizk, Y.M., and Schiff, L.B., "*Forebody Tangential Slot Blowing on an Aircraft Geometry*", Journal of Aircraft, Vol. 31, No. 4, 1994, pp. 922-928.

[5] Kandil, O A; Yang, Z; Sheta, E F, "*Flow control and modification for alleviating twin-tail buffet*", AIAA, Aerospace Sciences Meeting, 1998, AIAA-99-0138.

[6] Ferman, M.A., Liguore, S.L., Smith, C.M., and Colvin, B.J., "*Composite Exoskin Doubler Extends F-15 Vertical Tail Fatigue Life*", 34th Structures, Structural Dynamics, and Materials Conf., v. 1, 1993, pp. 398-407.

[7] Ashley, H., Rock, S.M., Digumarthi, R., Channey, K. and Eggers, A.J., "Active Control for Fin Buffet Alleviation", WL-TR-93-3099, 1994.

[8] Lazarus, K.B., Saarmaa, E., and Agnes, G.S., "Active smart material system for buffet load alleviation", Proc. SPIE, v. 2447, 1995, pp. 179-192.

[9] Moore, J.W., Spangler, R.L., Lazarus, K.B. and Henderson, D.A., "Buffet load alleviation using distributed piezoelectric actuators", Industrial and Commercial Applications of Smart Structures Technologies, ASME, AD v. 52, 1996, pp. 485-490.

[10] Hauch, R.M., Jacobs, J.H., Ravindra, K., and Dima, C., "Reduction of vertical tail buffet response using active control", J. of Aircraft, v. 33, n. 3, 1996, pp. 617-622.

[11] Nitzsche, F. ,Zimcik, D.G., and Langille, K., "Active control of vertical fin buffeting with aerodynamic control surface and strain actuation", 38th Structures, Structural Dynamics, and Materials Conf., v. 2, 1997, pp. 1467-1477.

[12] Moses, R.W., "Vertical-tail-buffeting alleviation using piezoelectric actuators: some results of the actively controlled response of buffet-affected tails (ACROBAT) program", Proc. SPIE, v. 3044, 1997, pp. 87-98.

[13] Hopkins, M; Henderson, D; Moses, R; Ryall, T; Zimcik, D; Spangler, R, "*Active vibration suppression systems applied to twin tail buffeting*", Smart structures and materials: Industrial and commercial applications of smart structures technologies, SPIE v. 3326, 1998, p. 27-33.

[14] Spangler, R.L., and Jacques, R.N., "*Testing of an active smart material system for buffet load alleviation*", 40th AIAA/ASME/ASCE/AHS/ASC Structures, Structural Dynamics, and Materials Conference, 1999, AIAA-99-1317.

[15] Nitzsche, F; Zimcik, DG; Ryall, TG; Moses, RW; Henderson, DA, "*Control law synthesis for vertical fin buffeting alleviation using strain actuation*", 40th AIAA/ASME/ASCE/AHS/ASC Structures, Structural Dynamics, and Materials Conference, 1999, AIAA-99-1317.

[16] Moses, R.W., "*Contributions to active buffeting alleviation programs by the NASA Langley Research Center*", 40th AIAA/ASME/ASCE/AHS/ASC Structures, Structural Dynamics, and Materials Conference, 1999, AIAA-99-1318.

[17] Pado, L. E., and Lichtenwalner, P. F., "*Neural predictive control for active buffet alleviation*", 40th

AIAA/ASME/ASCE/AHS/ASC Structures, Structural Dynamics, and Materials Conference, v. 2, 1999, pp. 1043-1053, (AIAA-99-1319).

[18] Hanagud, S; Bayon de Noyer, M; Luo, H; Henderson, D; Nagaraja, K.S., "*Tail buffet alleviation of high performance twin tail aircraft using piezo-stack actuators*", 40th AIAA/ASME/ASCE/AHS/ASC Structures, Structural Dynamics, and Materials Conference, v. 2, 1999, pp. 1054-1064, (AIAA-99-1320).

[19] Preumont, A., Dufour, J.P., and Malekian, C., "*Active Damping by a Local Force Feedback with Piezoelectric Actuators*", J. of Guidance, Control and Dynamics, Vol. 15, No. 2, 1992, pp. 390-395.

[20] Young, J.W., and Hansen, C.H., "*Control of Flexural Vibration in Stiffened Structures using Multiple Piezoceramic Actuators*", Applied Acoustic, Vol. 49, No. 1, 1996, pp. 17-48.

[21] Redmond, J., and Barney, P., "*Vibration Control of Stiff Beams and Plates Using Structurally Integrated PZT Stack Actuators*", J. of Intelligent Material Systems and Structures, Vol. 8, 1997, pp. 525-535.

[22] Mattice, M., La Vigna, C., "*Innovative Active Control of Gun Barrels Using Smart Materials*", Proc. SPIE, V 3039, 1997, pp. 630-641.

[23] Goh, C. J. and Caughey, T. K., "*On the stability problem caused by finite actuator dynamics in the collocated control of large space structures*", International Journal of Control, Vol. 41, No. 3,1985, pp. 787-802.

[24] Juang, J. N. and Phan, M., "*Robust Controller Designs for Second-Order Dynamic Systems: A Virtual Passive Approach*", Journal of Guidance, Control and Dynamics, Vol. 15, No. 5, 1992, pp. 1192-1198.

[25] Sim, E. and Lee, S. W., "*Active Vibration Control of Flexible Structures with Acceleration Feedback*", Journal of Guidance, Vol. 16, No. 2, 1993, pp. 413-415.

[26] Goh, C. J. and Yan, W. Y., "*Approximate Pole Placement for Acceleration Feedback Control of Flexible Structures*", Journal of Guidance, Vol. 19, No. 1, 1996, pp. 256-259.

[27] Bayon de Noyer, M., and Hanagud, S, "*Single Actuator and Multi-Mode Acceleration Feedback Control*", J. of Intelligent Material Systems and Structures, v 9, n 7, 1999, pp. 522-545.

[28] Bayon de Noyer, M., and Hanagud, S., "*Comparison of H_2 optimized design and cross-over point design for acceleration feedback control*". Collect Tech Pap, Struct. Struct. Dyn. Mater. Conf., v 4, 1998, pp. 3250-3258, AIAA-98-2091.

[29] Triplett, W.E., "*Pressure Measurements on Twin Vertical Tails in Buffeting Flow*", Journal of Aircraft, V. 20, N. 11, 1983, pp. 920-925.

[30] Komerath, N.M., Schwartz, R.J. and , Kim, J.M. "*Flow over a Twin-Tailed Aircraft at Angle of Attack, Part II: Temporal Characteristics*", Journal of Aircraft, V. 29, N. 4, 1992, pp. 553-558.

This page has been deliberately left blank

Page intentionnellement blanche